A Novel Unity Power Factor Hysteresis Current Control for SPMSM Using Switching Table

Mingdi Fan
School of Automation, Northwestern Polytechnical University, Xi'an, Shaanxi, 710072, P. R. China
Email: fanli1998@163.com

Hui Lin and Bingqiang Li
School of Automation, Northwestern Polytechnical University, Xi'an, Shaanxi, 710072, P. R. China
Email: {linhui, libingqiang}@nwpu.edu.cn

***Abstract*—In this paper, a novel unity power factor (UPF) hysteresis current control method for surface-mounted permanent magnet synchronous motor (SPMSM) drive system is presented. The optimum voltage vectors, which are selected from a switching table according to the magnitude and phase of the stator current vector, are applying to the voltage source inverter (VSI). The UPF operation for SPMSM is achieved by maintaining the angle between the stator current vector and stator flux vector at 90°. Compared with traditional direct torque control (DTC), the proposed method eliminates the disadvantages of the actual stator flux and torque estimation without deterioration of the dynamic properties of DTC. The current regulator is realized by using the hysteresis controller and the switching table while the vector control (VC) employs complicated coordinate rotating transformation, PI controller, and pulse width modulation (PWM). So, the proposed structure and the algorithm are easier to implement comparing with VC. It has been found that with the proposed scheme SPMSM drive shows adequate dynamic torque performance and considerable torque ripple reduction.**

***Index Terms*—unity power factor, permanent magnet synchronous motor, direct torque control, vector control, switching table, voltage source inverter**

I. INTRODUCTION

The permanent magnet synchronous motors (PMSMs) are popular in industrial AC motor drives due to high torque-to-current ratio, large power-to-weight ratio, high efficiency, high power factor and robustness, etc.

Two most widespread AC motor control schemes are vector control (VC) and direct torque control (DTC). The VC was invented for induction motors by Blaschke in 1972 [1], which is also known as field oriented control (FOC). Takahashi et al. [2] and Depenbrock [3] invented the DTC scheme for the control of induction motors in the mid of 1980's. In view of the successful application of the induction motor, VC [4-7] and DTC [8-10] have been applied to the PMSMs. Nowadays PMSM drives with VC and DTC are available on the market with several producers, different solutions and performance. Both VC and DTC can provide excellent static and dynamic performance for PMSM drive. However, their principles are significantly different. Reference [11] proposed the simulations of the motor dynamic response, parameter sensitivity and system complexity using VC and DTC respectively. The two control schemes were experimentally compared with a same hardware platform in Reference [12]. The simulations of the motor transient response and torque ripple were analyzed [13-15].

A unity power factor (UPF) control is of paramount importance in applications where energy saving and cost of electricity are critical, such as home appliances, fans, pumps, hybrid electric and electric vehicle motor drives [16]. Currently, the UPF operation for PMSM always utilizes VC [17, 18, 19]. Reference [17] designed a vector control system for PMSM based on stator flux orientation to obtain UPF. In Reference [18], based on controlling the d-axis stator current component, UPF operation method for PMSM was implemented using a digital signal processor (DSP) TMS320F2808 board, and power factor value was close to unity (greater than 0.94). A method of sensor-less VC with UPF for surface mounted permanent magnet synchronous motor (SPMSM) was presented in Reference [19].

Compared with VC, DTC has advantages as it is simple owing to the absence of PWM current controller and reference frame transformation, good robustness to parameter variation and external disturbances. Most importantly, it also has better dynamic response [20,21]. In the traditional DTC, the reference magnitude of the stator flux vector is a constant, which is approximately equal to the rotor flux magnitude. As a result, the power factor is low, approximately equal to 0.77 [22].

In this paper, based on the comparative analysis of the operation principle of VC and DTC, a stator current control scheme with switching table is presented, which ensures UPF operation for the PMSM drives. In the proposed algorithm, the magnitude of the stator current vector, the angle between the stator current vector and the stator flux vector, and the stator current vector position are used to select the optimum voltage switching vectors applying to the voltage source inverter. To achieve the speed control, only a PI controller, two hysteresis con-

Manuscript received June 14, 2013
Corresponding author: fanli1998@163.com

doi:10.4304/jcp.9.2.337-344

trollers, a switching table, two current sensors, and a speed sensor are required.

Some criteria to evaluate the performance of PMSM drives are proposed in this paper. They are used to compare the three control schemes (VC, DTC and the proposed control scheme) in both steady-state and transient operating conditions. For the sake of comparison, the three control schemes are implemented in the same simulation environment.

II. Control Schemes Analysis

Without loss of generality and for the sake of clarity, the following assumptions are made in the derivation [23]. 1) Saturation is neglected. 2) The induced EMF is sinusoidal. 3) Eddy currents and hysteresis losses are negligible. 4) There are no field current dynamics. 5) There is no cage on the rotor.

With these assumptions, the space vector diagram for PMSM is shown in Fig. 1, where $\alpha\beta$ is the two-phase stationary frame, dq is the two-phase rotary frame, $\vec{u_s}$ is the stator voltage vector, $\vec{i_s}$ is the current vector, $\vec{\psi_s}$ is the stator flux vector and $\vec{\psi_f}$ is the permanent magnet rotor flux vector, $\vec{E_s}$ is the electromotive force (EMF), L_s is the stator inductance, R_s is the stator winding resistance, p is the pair of poles, ω_r is the mechanical rotor angular speed, ω_e is the electrical rotor angular speed, θ_i is the phase of stator current in $\alpha\beta$ frame, θ_r is the rotor position angle, θ_s is the stator flux angle, δ is the load angle, γ is the torque angle and $\theta_{\psi i}$ is the flux current angle, i.e. the angle between stator current vector and stator flux vector.

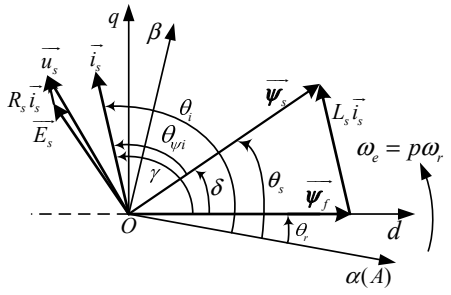

Figure 1. Space vector diagram for PMSM

The voltage and flux equations used to model PMSM in stationary frame can be derived as follows:

$$\vec{u_s} = R_s\vec{i_s} + \vec{E_s} = R_s\vec{i_s} + \frac{d\vec{\psi_s}}{dt} \tag{1}$$

$$\vec{\psi_s} = L_s\vec{i_s} + \vec{\psi_f} \tag{2}$$

$$\vec{E_s} = \vec{E_{si}} + \vec{E_{sm}} = L_s\frac{d\vec{i_s}}{dt} + j\omega_e\vec{\psi_s} \tag{3}$$

where: $L_s\frac{d\vec{i_s}}{dt}$ is the induced EMF ($\vec{E_{si}}$) and $j\omega_r\vec{\psi_s}$ is the motional EMF ($\vec{E_{sm}}$). Note that, the motional EMF is the product of rotor angular speed and stator flux.

Input to the VC or DTC is the reference torque T_e^*, which is set either by the user or by a superimposed control (e.g. speed control). The basic electromagnetic torque equations of SPMSM (for SPMSM: d-axis stator inductance is equal to q-axis stator inductance, i.e. $L_d = L_q = L_s$) for VC and DTC can be obtained as:

$$T_e = \frac{3}{2}p\left|\vec{\psi_f}\right|i_q = \frac{3}{2}p\left|\vec{\psi_f}\right|\left|\vec{i_s}\right|\sin\gamma \tag{4}$$

$$T_e = \frac{3}{2}p\frac{\left|\vec{\psi_f}\right|\left|\vec{\psi_s}\right|}{L_s}\sin\delta \tag{5}$$

Note that, for VC, as long as the amplitude and phase of the stator current vector are accurately controlled, the electromagnetic torque can be effectively controlled. For DTC, the control objects are the amplitude and phase of the stator flux vector.

As shown in Fig. 1, an orthogonal control grid, formed by the direct axis d and the quadrature axis q, is used in VC. The stator current is decomposed into two parts using coordinate transformation matrix (three-phase stationary frame ABC to two-phase rotary frame dq): d-axis stator current i_d and q-axis stator current i_q. i_d aligning with the rotor flux vector $\vec{\psi_f}$ may be seen as the flux-producing current, and i_q which has perpendicular phase relationship with $\vec{\psi_f}$ may be seen as the torque-producing current. The regulators of i_d and i_q are usually enforced through the inverter with one of the popular methods: hysteresis control, pulse width modulation (PWM), and space vector modulation (SVM). Therefore, the VC is exploited to make the PMSM drive system a high-performance drive system with independent control of its stator flux and electromagnetic torque.

Unlike VC, the DTC does not require any current regulators, coordinate transformation, PWM or SVM. The principle of DTC is to directly select voltage vectors according to the difference between the reference and the actual value of the torque and the flux linkage. Thus, the torque and flux errors are compared in hysteresis comparators respectively. Depending on the comparators a voltage vector is selected from the switching table. In spite of its simplicity, DTC allows a good torque control in steady-state and transient operating conditions to be obtained. Compared to VC, DTC might be preferred for high dynamic applications, but it shows higher current and torque ripple. The performance of DTC strongly depends on the quality of the estimation of the actual stator flux and torque.

The proposed scheme in this paper utilizes the magnitude of the stator current vector, the angle between the stator current vector and the stator flux vector, and the

stator current position to select the optimum voltage switching vectors from the switching table. Similar to VC, the basic idea is to control the amplitude and phase of stator current vector. Similar to DTC, it is based on the two-phase stationary frame without PWM and SVM as well as without decoupling of the stator current. The stator current vector is regulated through the selection of optimum space voltage vectors from the switching table with two hysteresis controllers, and then excellent dynamic torque response is achieved. The new control scheme can eliminate the disadvantages of depending on the actual stator flux and torque estimation without deterioration of the dynamic properties of DTC.

The basic electromagnetic torque equations of SPMSM for the proposed scheme can be alternately derived as:

$$T_e = \frac{3}{2} p \left|\overrightarrow{\psi_f}\right| \left|\vec{i}_s\right| \sin\gamma = \frac{3}{2} p \left|\overrightarrow{\psi_s}\right| \left|\vec{i}_s\right| \sin\theta_{\psi i} \tag{6}$$

The relative position between stator current vector $\vec{i}_s$ and the stator flux vector $\overrightarrow{\psi_s}$ are shown in Fig. 1. $\theta_{\psi i}$ is the angle between the $\vec{i}_s$ and $\overrightarrow{\psi_s}$. A control strategy can be synthesized to keep the flux current angle $\theta_{\psi i}$ at 90°. The EMF vector $\overrightarrow{E_s}$ leads $\overrightarrow{\psi_s}$ by 90°. Controlling $\vec{i}_s$ to lead $\overrightarrow{\psi_s}$ by the same angle results in the coincidence of $\overrightarrow{E_s}$ and $\vec{i}_s$. If the stator resistance R_s is neglected, the stator terminal voltage will be equal to $\left|\overrightarrow{E_s}\right|$, and the relative phase between them is zero. Therefore, the angle between the stator current vector and stator voltage vector is zero, resulting in the UPF operation of the SPMSM drive.

III. UPF- Hysteresis Current Control

A. Stator Current Vector

In proposed stator current direct control, the parameters are calculated in the $\alpha\beta$ two-phase stationary frame. The stator current i_α and i_β can be obtained by i_A and i_B measured by current sensors using coordinate transformation matrix as [24]:

$$\begin{bmatrix} i_\alpha \\ i_\beta \\ i_0 \end{bmatrix} = \frac{2}{3} \begin{bmatrix} 1 & -1/2 & -1/2 \\ 0 & \sqrt{3}/2 & -\sqrt{3}/2 \\ 1/2 & 1/2 & 1/2 \end{bmatrix} \begin{bmatrix} i_A \\ i_B \\ -i_A - i_B \end{bmatrix} \tag{7}$$

where: i_A and i_B are stator phase current, i_α and i_β are stator current in $\alpha\beta$ frame. i_0 is zero-sequence current. Then the amplitude and phase of the stator current are derived as [24]:

$$\left|\vec{i}_s\right| = \sqrt{i_\alpha^2 + i_\beta^2} \tag{8}$$

$$\theta_i = \arctan\frac{i_\beta}{i_\alpha} \tag{9}$$

As shown in Fig. 1, the flux current angle $\theta_{\psi i}$ can be derived as:

$$\theta_{\psi i} = \gamma - \delta = \theta_i - \theta_r - \arcsin\frac{L_s\left|\vec{i}_s\right|}{\left|\overrightarrow{\psi_f}\right|} \tag{10}$$

To achieve the UPF, the flux current angle should be controlled at 90º, so the reference torque angle γ^* is related with the load angle δ as:

$$\gamma^* = \delta + \frac{\pi}{2} = \arcsin\frac{L_s\left|\vec{i}_s\right|}{\left|\overrightarrow{\psi_f}\right|} + \frac{\pi}{2} \tag{11}$$

B. Voltage Vector Selection

According to (1) and (3), the derivative of the stator current vector can be derived as:

$$\frac{d\vec{i}_s}{dt} = \frac{\vec{u}_s - R_s\vec{i}_s - j\omega_e\overrightarrow{\psi_s}}{L_s} \tag{12}$$

which determines the direction and the rate of the stator current vector change. Graphical illustration of formula (12) is shown in Fig 2.

$\overrightarrow{E_{sm}}$ is the motional EMF which can be obtained by multiplying the mechanical rotor angular speed by stator flux. As shown in Fig. 2, the effect of stator voltage vector on stator current vector in proposed control scheme is similar to the effect of stator voltage vector on stator flux vector in DTC, i.e. the direction of the derivative of the stator current is the same with the set stator voltage vector, under the condition that the motional EMF is zero (motor speed is zero), or can be ignored. However, usually the motional EMF cannot be ignored; so the direction of the derivative of the stator current will not be the same with the set stator voltage vector. When the motor speed is high, due to the presence of the motional EMF, the stator voltage vector selection may be unable to make $\left|\vec{i}_s\right|$ and γ increase at the same time, and may also be unable to make $\left|\vec{i}_s\right|$ increase and γ decrease. In order

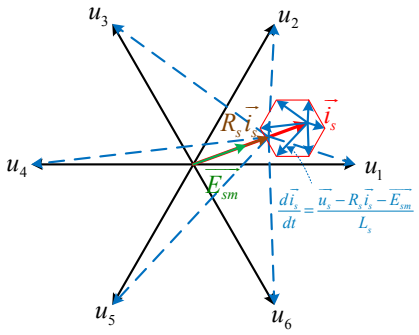

Figure 2. Typical moving direction of current vector locus

to specifically analyze the effect of stator voltage vector on the amplitude and phase of the stator current vector in the presence of motional EMF, the stator current vector

locating between the stator voltage vector u_1 and u_2 is taken for an example, as shown in Fig. 3.

According to Fig. 3, the stator current vector is located between the stator voltage vectors u_1 and u_2, O is the starting point of $\overrightarrow{E_{sm}}$, u_1 and u_2. E and D are the respective terminal points of u_1 and u_2. A and C are the respective midpoints of u_2 and u_1. Taking A as the center and OD as the diameter, the purple circle is drawn. As the angle inscribed in a semicircle is always a right angle, if the terminal of $\overrightarrow{E_{sm}}$ is located in this purple circle, the magnitude of the stator current vector will be increased by u_2 and vice versa. Similarly, Taking A as the center and OE as the diameter, the brown circle is drawn. If the terminal of $\overrightarrow{E_{sm}}$ is located in this brown circle, the magnitude of the stator current vector will be increased by u_1 and vice versa. The $\overrightarrow{E_{sm}}$ of a rated speed PMSM motor is normally equal to $(0.35 \sim 0.85)\left|\overrightarrow{u_s}\right|$ [24]. It means that the terminal of $\overrightarrow{E_{sm}}$ usually does not exceed the area (O-A-D-B-E-C-O).

Based on the above analysis, this area can be divided into the following three sub area. Area I (O-A-B-C-O): if the terminal of $\overrightarrow{E_{sm}}$ is located in area I, u_2 can make the current vector amplitude and γ increase, while u_1 can make the current vector amplitude increase and γ decreases. Area II (A-D-B-A): if the terminal of $\overrightarrow{E_{sm}}$ is located in area II, u_2 can make the current vector amplitude and γ increase which is similar with in area I, but u_1 will make the current vector amplitude and γ decrease. Area III (C-B-E-C): if the terminal of $\overrightarrow{E_{sm}}$ is located in area III, u_1 can make the current vector amplitude increase and γ decrease which is similar with in area I, but u_2 will make the current vector amplitude decrease and γ increase.

In this paper, a twelve sectors control method of stator current vector is presented for the construction of the switching table. The twelve sectors are shown in Fig. 4.

As discussed before, the voltage vector switching table is adopted, as presented in Table I. In order to discuss the reasonability of Table I, taking the sector θ_1 as example, u_2 will make the current vector amplitude decrease and γ increase where the terminal of $\overrightarrow{E_{sm}}$ is located in area III as shown in Fig. 3(c). Although that is not suitable with the outputs of the hysteresis controllers, considering the discrete nature of the VSI, u_2 is still the best choice compared with the other voltage vectors. Furthermore, from Fig. 3(c) we can see that, u_2 makes the current vector amplitude decrease slowly and it will make γ increase quickly to reach the upper limit of the hysteresis controller, and then u_1 should be chosen to increase the current vector amplitude. Sectors $\theta_2 \sim \theta_{12}$ are similar with sector θ_1. So setting the hysteresis controllers reasonable, the current will be well regulated by selecting voltage vectors from Table I.

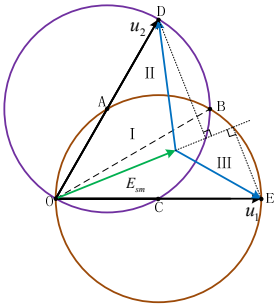

I (O-A-B-C-O)

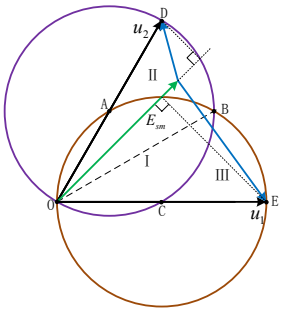

(b) II (A-D-B-A)

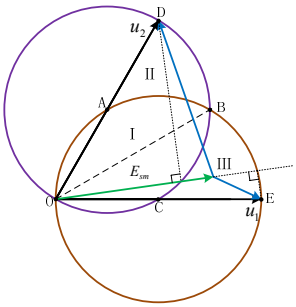

(c) III (C-B-E-C)

Figure 3. Effect of stator voltage vector on stator current vector

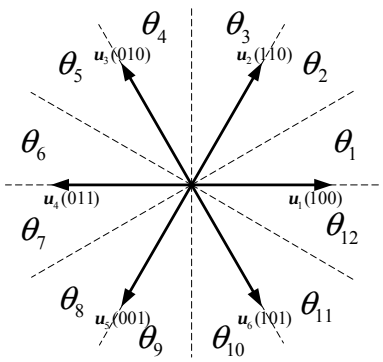

Figure 4. Sectors partition for current vector

TABLE I.
SWITCHING TABLE OF VOLTAGE VECTORS

H_i	H_γ	θ_1	θ_2	θ_3	θ_4	θ_5	θ_6	θ_7	θ_8	θ_9	θ_{10}	θ_{11}	θ_{12}
1	1	$\boldsymbol{u}_2$	$\boldsymbol{u}_2$	$\boldsymbol{u}_3$	$\boldsymbol{u}_3$	$\boldsymbol{u}_4$	$\boldsymbol{u}_4$	$\boldsymbol{u}_5$	$\boldsymbol{u}_5$	$\boldsymbol{u}_6$	$\boldsymbol{u}_6$	$\boldsymbol{u}_1$	$\boldsymbol{u}_1$
	0	$\boldsymbol{u}_1$	$\boldsymbol{u}_1$	$\boldsymbol{u}_2$	$\boldsymbol{u}_2$	$\boldsymbol{u}_3$	$\boldsymbol{u}_3$	$\boldsymbol{u}_4$	$\boldsymbol{u}_4$	$\boldsymbol{u}_5$	$\boldsymbol{u}_5$	$\boldsymbol{u}_6$	$\boldsymbol{u}_6$
0	1	$\boldsymbol{u}_3$	$\boldsymbol{u}_4$	$\boldsymbol{u}_4$	$\boldsymbol{u}_5$	$\boldsymbol{u}_5$	$\boldsymbol{u}_6$	$\boldsymbol{u}_6$	$\boldsymbol{u}_1$	$\boldsymbol{u}_1$	$\boldsymbol{u}_2$	$\boldsymbol{u}_2$	$\boldsymbol{u}_3$
	0	$\boldsymbol{u}_5$	$\boldsymbol{u}_6$	$\boldsymbol{u}_6$	$\boldsymbol{u}_1$	$\boldsymbol{u}_1$	$\boldsymbol{u}_2$	$\boldsymbol{u}_2$	$\boldsymbol{u}_3$	$\boldsymbol{u}_3$	$\boldsymbol{u}_4$	$\boldsymbol{u}_4$	$\boldsymbol{u}_5$

C. Control Diagram

The control diagram of the proposed control scheme is shown in Fig. 5.

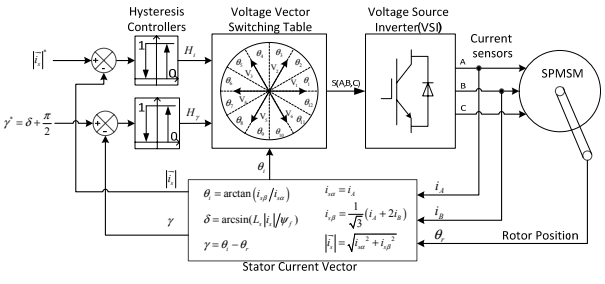

Figure 5. Control diagram of the presented scheme

The proposed control scheme can be described as follows:

- The amplitude and phase of the stator current vector is obtained using current sensors and speed sensor by (7) (8) (9) and (10).
- The reference amplitude of stator current is set either by the user or by a superimposed control.
- To achieve the UPF, the reference torque angle γ^* is obtained from (11).
- The equation (12) describes the derivative of the stator current vector.
- The inputs of the hysteresis controllers are the difference between the reference and the actual value of the stator current amplitude and the torque angle. Depending on the outputs of hysteresis controllers a voltage vector is selected from the switching table (Table I).
- The electromagnetic torque can be calculated from (6).

IV. RESULTS AND DISCUSSION

In order to investigate the performance of SPMSM drive under VC, DTC or the presented scheme, simulation models are constructed using Matlab/Simulink software package. Three control schemes are implemented in the same SPMSM drive using the same implementation conditions.

The step size of simulation time is 5μs.

The SPMSM is Y-connected with parameters as in Table II. The VSI used in simulation is IGBT inverter with +150 to -150 dc link voltage. The maximum switching frequency of the IGBT is set at 10 kHz.

TABLE II.
PARAMETERS OF SPMSM USED FOR SIMULATION

Rated DC voltage	U_n	*300 (V)*
Rated speed	ω_n	*2000 (r/min)*
Rated torque	T_{en}	*8 (Nm)*
Number of pole pairs	p	*4*
Stator winding resistance	R_s	*0.9585 (Ω)*
Stator inductance	L_s	*5.25 (mH)*
Permanent magnet flux	ψ_f	*0.1827 (Vs)*
Moment of inertia	J	*0.0006329 (kgm²)*
Friction constant	B	*0.0 (Nms)*

The speed loop proportional and integral parameters (in parallel PI form) of DTC are 0.2 and 0.5 respectively. The band width of the torque hysteresis controller is 0.05Nm, and the band width of the flux hysteresis controller is 0.001Vs.

The VC control scheme is based on the control strategy i_d=0. The speed loop proportional and integral parameters are 0.1 and 100 respectively. The d, q axis current loops proportional and integral parameters are 100 and 50 respectively.

The proposed control scheme is based on the control strategy UPF. The speed loop proportional and integral parameters are 0.1 and 50 respectively. The band width of the current hysteresis controller is 0.05A, and the band width of the torque angle hysteresis controller is 2º.

In order to compare the performance of the proposed with DTC and VC, the following criteria are selected.

Power factor (PF), power ripple factor (PRF) and copper losses (P_{Cu}) are the criteria that concern the power performance, such that:

$$PF = \frac{P}{\sqrt{P^2 + Q^2}} = \frac{P}{S} \tag{13}$$

$$PRF = \frac{P_{\max} - P_{\min}}{P_{mean}} \times 100\% \tag{14}$$

$$P_{Cu} = 1.5 * R_s \left| \vec{i_s} \right|^2 \tag{15}$$

where: P is the active power, Q is the reactive power, S is the apparent power. In this paper, the 3-phase instantaneous active power P and reactive power Q are calculated using the following equations [25]:

$$P = V_a * I_a + V_b * I_b + V_c * I_c \tag{16}$$

$$Q = \frac{\sqrt{3}}{3}(V_{bc} * I_a + V_{ca} * I_b + V_{ab} * I_c) \tag{17}$$

where: V_a, V_b and V_c are the instantaneous stator phase voltages; V_{ab}, V_{bc} and V_{ca} are the instantaneous stator line voltages; I_a, I_b and I_c are the instantaneous stator

phase currents. In a Y-connected SPMSM, the phase currents are equal to the line currents.

Torque ripple factor (TRF) and torque per ampere rate (TPA) are the criteria that concern the torque performance of the SPMSM drives, such that:

$$TRF = \frac{T_{e\_\max} - T_{e\_\min}}{T_{e\_mean}} \times 100\% \tag{18}$$

$$TPA = T_e \Big/ \left|\vec{i}_s\right| \tag{19}$$

The simulation results of the three control schemes are shown in Fig. 6 and Fig. 7. The power performance is simulated with 2000r/min closed speed loop, 8Nm load torque, while torque dynamic response is simulated with open speed loop. The active power, reactive power and copper losses of the three control schemes are shown in Fig. 6. The power factors and power ripple factors can be calculated from (13) and (14), and the power performance is shown in table III. The striking feature is the low apparent power requirement in the proposed control, as the stator flux linkages decrease with stator current increasing, limiting the stator voltage requirement.

Fig. 7(a), (b) and (c) show the torque performance of the SPMSM drive with VC (i_d=0), DTC and the proposed control scheme respectively. Note that, the rise time of the motor torque from 2Nm to 8Nm with VC is 2.46ms, while it is 1.11ms with DTC, and 1.40ms with the proposed control. The TRF and TPA can be calculated from (18) and (19). The TRF has the amplitude of 8.1 percent in the case of the VC, and 13.5 percent in the case of the DTC, while no more than 10.4 percent in the case of the proposed control. So the proposed control scheme is a tradeoff between torque ripple and torque dynamic, which shows lower torque ripple similar to VC and excellent torque dynamic similar to DTC.

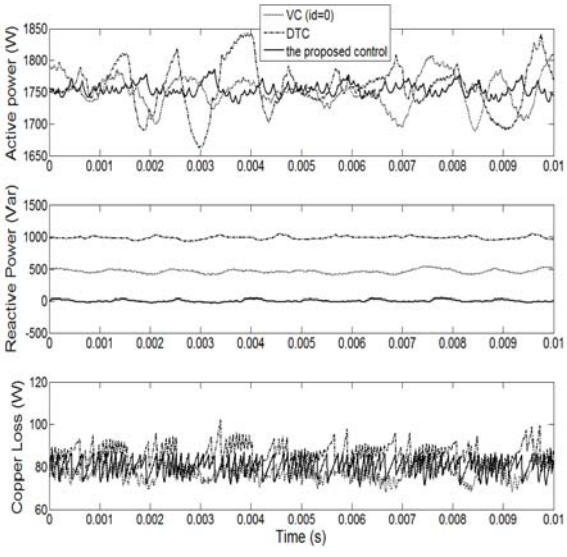

Figure 6. Power performance with rated load torque

TABLE III.
POWER PERFORMANCE OF SPMSM

	P (W)	Q (Var)	S (VA)	PF	PRF	P_{Cu} (W)
VC	1751.9	463.1	1812.1	0.967	6.9%	76.4
DTC	1758.3	985.7	2015.8	0.872	10.3%	82.8
proposed	1754.3	3.7	1754.3	1.00	3.1%	78.8

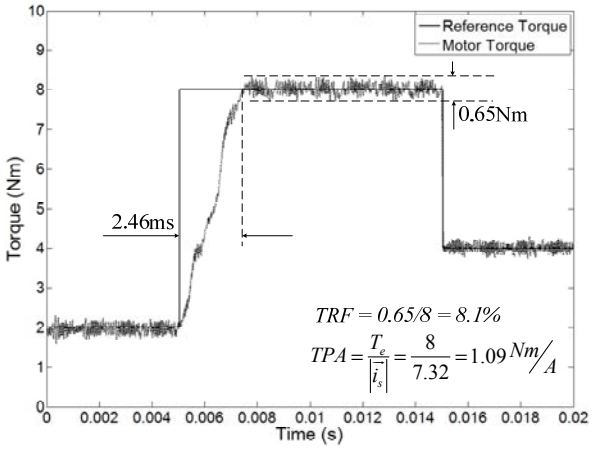

(a) VC (i_d=0)

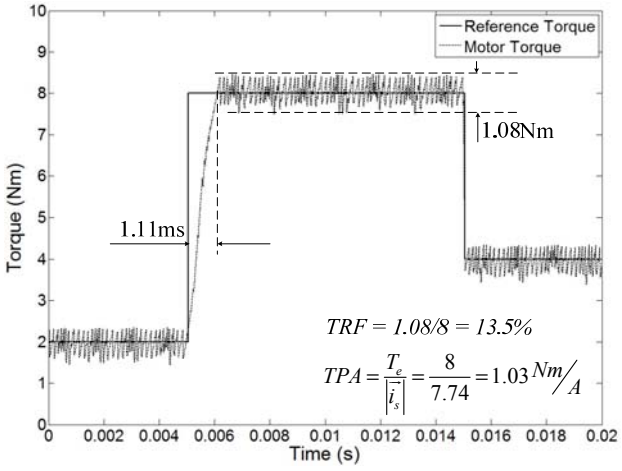

(b) DTC

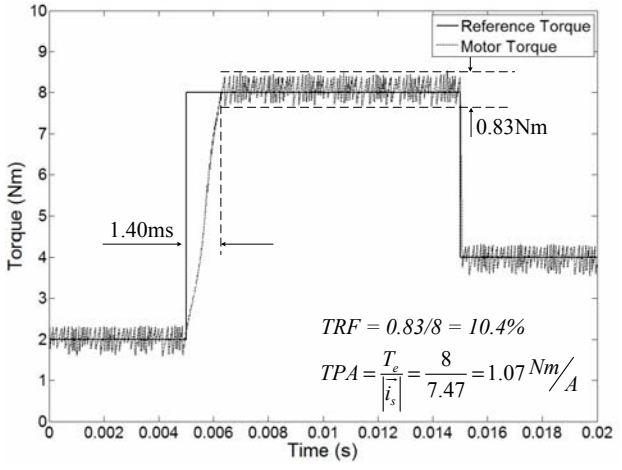

(c) The proposed control

Figure 7. Torque dynamic response with open speed loop

As shown in Fig. 7, the TPA of VC, DTC and the proposed control are 1.09Nm/A, 1.03Nm/A and 1.07Nm/A respectively. The TPA of VC is more than the others, because the VC control scheme is based on the control strategy i_d=0 which results in the maximum torque per ampere operation in SPMSM.

As shown in Fig. 6, Fig. 7 and Table III, the proposed control scheme improves the torque dynamic performance without deterioration of the torque smoothness properties of VC, and as compared with DTC, it shows considerable torque ripple reduction, and achieves UPF to improve the power performance. Because of the difference in power factor, for equivalent power output, it can be inferred that the proposed control will have apparent power compared to the other two. Lower apparent power means lower volt–amp rating of the inverter, lower volume filter, and higher efficiency in SPMSM drives as compared with the other two.

Fig. 8 and Fig. 9 show the transient response and steady states of the proposed control with 2000 r/min

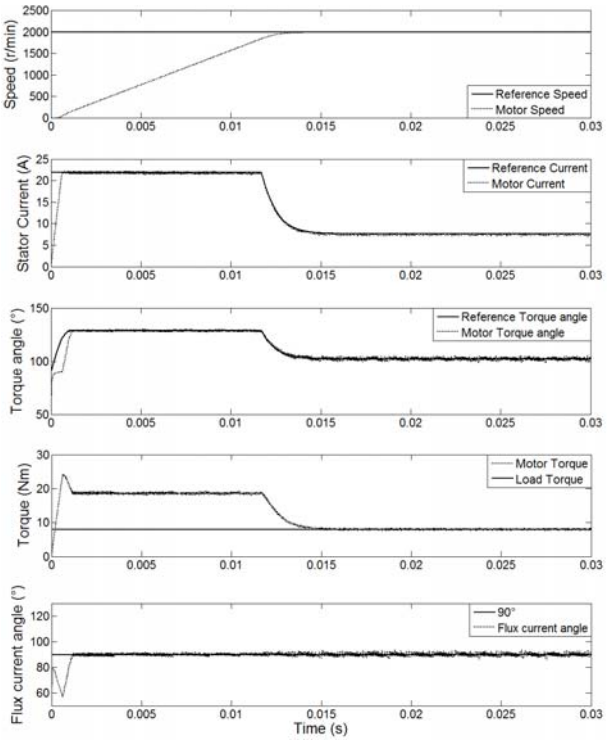

Figure 8. Steady state of SPMSM with the presented control

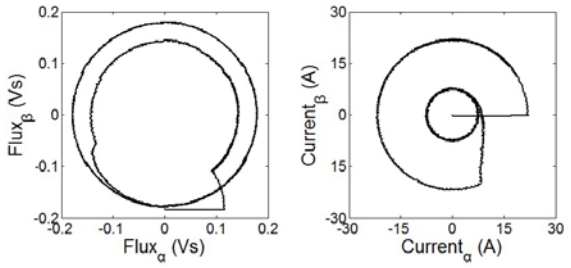

Figure 9. Locus circle of the stator flux and current with the presented control

closed speed loop, and 8Nm load torque. It is noticed that with the proposed control, the motor current is fully controlled to track its reference curve both at transient response and steady states, and the flux current angle is fixed at 90° which can make the SPMSM drive achieve UPF.

V. CONCLUSION

To achieve the high-performance of PMSM drive system, the stator current control based on UPF is presented. The basic idea of the control is to calculate the parameters in the two-phase stationary frame, regulate the magnitude and the phase of the stator current vectors in hysteresis controllers by choosing proper voltage vectors from the switching table. So that satisfactory dynamic response of the torque and UPF can be expected.

The proposed control scheme implements the current regulator without decoupling the stator currents, throwing aside the complicated coordinate rotating transformation. The essential parameters are stator currents of three phases and the rotor position. As a result, the structure and the algorithm of the proposed control scheme are simple and easy to implement.

The simulation results of the proposed control scheme show that the SPMSM drive system has good performance during transient response and steady-state operations. It is a combination of the advantages of VC and DTC, and it can be applied to the servo systems that high precision, high dynamic and high power factor are needed.

REFERENCES

[1] Blaschke, F., "The principle of field orientation as applied to the new transvector closed loop control system for rotating field machines", *Siemens Review*. Vol. 34: 217 – 220. 1972.

[2] Takahashi, I. and Noguchi, N., "A new quick response and high efficiency control strategy of an induction motor", *IEEE Trans. Ind. Application,* Vol. 22, pp. 820-827. 1986.

[3] Depenbrock, M., "Direct self-control (DSC) of inverter-fed induction machine", *IEEE Transactions on Power Electronics*, Vol. 3 No. 4, pp.420-429. 1988.

[4] Mademlis, C. and Margaris, N., "Loss minimization in vector controlled interior permanent magnet synchronous motor drive", *IEEE Trans. On Indus. Electron.,* Vol. 49 No. 6, pp. 1344-1347. 1992.

[5] Konghirun, M., "A resolver based vector control drive of permanent magnet synchronous motor on a fixed point digital signal processor", *Proc. IEEE-TENCON'* 2004, pp. 1316-1320. 2004.

[6] Janiszewski, D and Muszynski, R., "Sensorless control of PMSM drive with state and load torque estimation", *COMPEL,* Vol. 26 Iss: 4, pp. 1175-1187. 2007.

[7] Wang, BJ and Wang JJ. "Sliding mode control of surface-mount permanent-magnet synchronous motor based on error model with unknown load", *Journal of Software*, V6, n5, pp. 819-825, 2011

[8] Tang, L., Zhong, L., Rahman, M.F. and Hu, Y, "Novel Direct Torque Controlled Interior Permanent Magnet Synchronous Machine Drive With Low Ripple in Flux and Torque and Fixed Switching Frequency", *IEEE*

Trans., Power Electron., Vol. 19, No.2, pp. 346-354. 2004.

[9] Uddin, M. N., Radwan, T. S., George, G. H. and Rahman, M. A., "Performance of current controllers for VSI fed IPMSM drive", *IEEE Trans. on Industry Applications,* Vol. 36 No. 6, pp. 1531-1538. 2000.

[10] Adam, A. A. and Gulez, K., "A new sensorless hysteresis direct torque control algorithm for PMSM with minimum torque ripples", *COMPEL,* Vol. 28 Iss: 2, pp. 437-453. 2009.

[11] Le-Huy, H., "Comparison of field oriented control and direct torque control for induction motor drives", *IEEE-IAS Conference on Industry Applications, IEEE 1999*, pp. 1245-1252. 1999.

[12] Telford, D., Dunnigan, M. W. and Williams, B. W. A., "A comparison of vector control and direct torque control of an induction machine", *IEEE Power Electronics Specialists Conference*, *IEEE 2000,* pp. 421-426. 2000.

[13] Casadei, D., Profumo, F., Serra, G. et al., "FOC and DTC: two variable schemes for induction motors torque control", *IEEE Transactions on Power Electronics,* Vol. 17 No 5, pp. 779-787. 2002.

[14] Cruz, C., Gallegos, M, A., Alvarez, R. et al., "Comparison of several nonlinear controllers for induction motors", *IEEE International Power Electronics Congress, IEEE 2004*, pp. 134-139. 2004.

[15] Souad, R. and Zeroug, H., "Comparison between direct torque control and vector control of a permanent magnet synchronous motor drive", *IEEE International Power Electronics and Motion Control Conference, IEEE 2008,* pp.1209-1214. 2008.

[16] Krishnan R. *Permanent magnet synchronous and brushless DC motor drives*. Taylor & Francis Group. 2010.

[17] Liu WL and Zhang GZ. "Unity Power Factor Control of Permanent Magnet Synchronous Motor". *Micromotors*. 45(2): 63 - 67. 2012.

[18] Pham, D. C., Huang, SD., Huang, KY. and Cheng, SY. "Unity power factor control in sensorless PMSM drive systems: A DSP-based implementation approach". *ICIC Express Letters,* Part B: Applications. 3(2): 383 - 388. 2012.

[19] Wu F, Wan SM and Huang SH. "Unity power factor control for PMSM position sensor-less drive". *11th International Conference on Electrical Machines and Systems, ICEMS 2008*. Wuhan, China. 1618 – 1620. 2008.

[20] Dwivedi S. and Singh B. "Vector control Vs Direct Torque Control comparative evaluation for PMSM drive". *2010 Joint International Conference on Power Electronics, Drives and Energy Systems, PEDES 2010 and 2010 Power India*. New Delhi, India. 2010.

[21] Cai BJ and Nian XH "A novel MC-DTC method for induction motor based on fuzzy-neural network space vector modulation", *Journal of Software*, V7, n5, pp. 966-973, 2012

[22] Ozturk S. B. "Direct torque control of permanent magnet synchronous motors with non-sinusoidal back-EMF". Ph.D. Texas A&M University. Texas, United States. 2008.

[23] Pillay, P. and R. Krishnan. "Modeling, simulation, and analysis of permanent-magnet motor drives. I. The permanent-magnet synchronous motor drive", *IEEE Transactions on Industry Applications*, Vol. 25 No. 2, pp. 265-273. 1989.

[24] Li, B. and Lin, H., "Direct Control of Current Vector for Surface-mounted Permanent Magnet Synchronous Motor", *Proceedings of the CSEE,* Vol.31, pp. 288-294. 2011.

[25] Fang Zheng, P. and L. Jih-Sheng. "Generalized instantaneous reactive power theory for three-phase power systems." *IEEE Transactions on Instrumentation and Measurement,* 45(1): 293-297. 1996.

Mingdi Fan was born in HeZe City, Shandong, China, in 1987. He obtained bachelor degree in Northwestern Polytechnical University, China, in 2008. From 2010 to 2011, he worked as a visiting scholar in Kassel University, Germany. He is now a doctoral student at Northwestern Polytechnical University. His major research fields are AC servos, nonlinear motor control and wind power technology.
E-mail: fanli1998@163.com

Hui Lin was born in 1957. He received the Ph.D. degree in control theory and applications from Northwestern Polytechnical University in 1993. From 1989 to 1990, he worked as a visiting scholar in University of Braunschweig, Germany. From 2003 to 2004, he worked as a visiting scholar in University of Michigan, USA. Now, he works as a professor and Ph.D. supervisor in Northwestern Polytechnical University. His research interests include iterative learning control, control theory and control engineering, and motion control technology.
E-mail: linhui @nwpu.edu.cn

Bingqiang Li was born in 1982. He received the M.S. degree in power electronics and power drives and Ph.D. degree in control science and engineering from Northwestern Polytechnical University in 2007 and 2010, respectively. From 2010 to 2012, he worked as a post-doctor in Postdoctoral Research Station of Electrical Engineering in Northwestern Polytechnical University. Now, he works as a lecturer in Northwestern Polytechnical University. His research interests include iterative learning control, power electronics and power drives, and AC servos.
E-mail: libingqiang@nwpu.edu.cn